# HITTITE JOURNAL OF SCIENCE AND ENGINEERING

e-ISSN: 2148-4171 Volume: 12 • Number: 3 September 2025

# Tailoring Graphene Quantum Dots through the Pyrolysis of Citric Acid, Phenylalanine, and Tryptophan: Effect of Precursor Ratios on Synthesis Efficiency and Properties

# Recep Üzek 💿

Hacettepe University, Department of Chemistry, 06800, Ankara, Türkiye.

# **Corresponding Author**

### Recep Üzek

E-mail: ruzek@hacettepe.edu.trPhone: +90 312 297 7169 RORID: https://ror.org/04kwvgz42

## **Article Information**

**Article Type:** Research Article **Doi:** https://doi.org/10.17350/HJSE19030000358

**Received:** 25.02.2025 **Accepted:** 03.07.2025 **Published:** 30.09.2025

#### Cite As

Üzek R. Tailoring Graphene Quantum Dots through the Pyrolysis of Citric Acid, Phenylalanine, and Tryptophan: Effect of Precursor Ratios on Synthesis Efficiency and Properties . Hittite J Sci Eng. 2025;12(3):121-127.

**Peer Review:** Evaluated by independent reviewers working in at least two different institutions appointed by the field editor.

**Ethical Statement:** Not available. **Plagiarism Checks:** Yes - iThenticate

**Conflict of Interest:** Authors approve that to the best of their knowledge, there is not any conflict of interest or common interest with an institution/organization or a person that may affect the review process of the paper.

### **CREDIT AUTHOR STATEMENT**

**Recep ÜZEK:** Conceptualization, Methodology, Software, Validation, Writing- original draft, Data curation, Visualization, Investigation, Supervision, Writing-review and editing.

**Copyright & License:** Authors publishing with the journal retain the copyright of their work licensed under CC BY-NC 4.

# Tailoring Graphene Quantum Dots through the Pyrolysis of Citric Acid, Phenylalanine, and Tryptophan: Effect of Precursor Ratios on Synthesis Efficiency and Properties

Recep Üzek

Hacettepe University, Department of Chemistry, 06800, Ankara, Türkiye.

#### Abstract

Graphene Quantum Dots (GQDs) are gaining significant attention due to their unique optical, electronic, and biocompatible properties, making them ideal candidates for applications in bioimaging, sensing, and drug delivery. This study explores the synthesis of GQDs derived from citric acid (CA), phenylalanine (Phe), and tryptophan (Trp) using a pyrolysis method, where GQDs were synthesized using 2.0 g of CA with varying amounts of Phe (0.75 g, 0.50 g, 0.25 g) and Trp (0.25 g, 0.50 g, 0.75 g), corresponding to GQDs1, GQDs2, and GQDs3, respectively. The influence of precursor composition on the structural, optical, and physicochemical properties of GQDs was analyzed. Particle size measurements showed a hydrodynamic diameter range of 0.89 nm to 1.5 nm, with increasing Trp content leading to larger particles and a broader size distribution, reflected in polydispersity index (PDI) values of 0.221, 0.312, and 0.368 for GQDs1, GQDs2, and GQDs3, respectively. Zeta potential analysis revealed values of -21.4 mV, -12.2 mV, and -7.5 mV for GQDs1, GQDs2, and GQDs3, respectively, indicating reduced surface charge with higher Trp content, which may affect colloidal stability. Optical characterization showed  $\pi \rightarrow \pi^*$  (-230-270 nm) and  $n \rightarrow \pi^*$  (-300-350 nm) transitions in the UV-Vis spectra, with varying absorbance intensities across samples. Fluorescence spectroscopy confirmed strong emission properties, which were highly dependent on precursor ratios. Quantum yield (QY) values were 32.2%, 95.5%, and 75.6% for GQDs1, GQDs2, and GQDs3, respectively, highlighting the role of nitrogen doping in fluorescence enhancement. These findings demonstrate that controlled precursor composition can fine-tune GQD properties, offering potential for optoelectronic, bioimaging, and sensing applications. Further exploration of functionalization strategies could enhance their practical utility.

Keywords: Graphene quantum dots, pyrolysis, quantum yield, fluorescence

#### **INTRODUCTION**

Graphene Quantum Dots (GQDs), a rising star in nanotechnology, have drawn considerable attention due to their unique properties and wide-ranging applications. These zerodimensional carbon-based nanomaterials exhibit exceptional optical properties, including strong photoluminescence, high photostability, and tunable fluorescence emission, alongside excellent biocompatibility, chemical stability, and eco-friendliness  $^{1-3}$ . GQDs are also characterized by quantum confinement and edge effects, making them highly versatile for applications in bioimaging, chemical sensing, drug delivery, energy storage, and environmental monitoring <sup>1,4,5</sup>. Compared to traditional semiconductor quantum dots, GQDs offer significant advantages such as low toxicity, sustainable production routes, and compatibility with biological systems, positioning them as promising candidates for next-generation nanomaterials <sup>6</sup>.

Recent studies have highlighted the expanding frontiers of GQD research across various disciplines 7-10. For instance, Saeidi et al. demonstrated the use of nitrogen-doped GQDs for enhancing the performance of perovskite solar cells, achieving significant improvements in power conversion efficiency 11. In the realm of biomedicine, Huang et al. developed multifunctional GQDs for targeted drug delivery and bioimaging, leveraging their ability to simultaneously transport drugs and provide fluorescence tracking 12. Environmental applications have also gained traction, as evidenced by Anusuya et al., who synthesized GQDs for the detection of toxic heavy metal ions like mercury and lead, achieving detection limits in the nanomolar range <sup>13,14</sup>. These advancements underline the critical importance of tailoring GQD properties to meet application-specific requirements. The synthesis of GQDs is a key determinant of their properties, with methods such as hydrothermal treatment, chemical oxidation, and pyrolysis being widely explored <sup>6,15,16</sup>. Among these, pyrolysis stands out as an efficient, scalable, and cost-effective method for synthesizing GQDs with

tunable properties <sup>17</sup>. Organic precursors such as citric acid, glucose, and amino acids are particularly advantageous in pyrolytic synthesis due to their natural abundance and their ability to introduce functional groups that enhance GQD performance. Citric acid, for example, serves as a reliable carbon source while also imparting carboxylic functional groups that improve water dispersibility <sup>18</sup>. Amino acids like phenylalanine and tryptophan, on the other hand, provide nitrogen doping and aromatic structures, which are known to enhance fluorescence quantum yield, stability, and electronic properties.

Despite substantial progress, there remains a critical gap in understanding the role of precursor composition in determining GQD properties. Most studies have focused on single or binary precursors, with limited exploration of multicomponent precursor systems <sup>19-21</sup>. The combination of citric acid with amino acids like phenylalanine and tryptophan presents a unique opportunity to systematically investigate the effects of precursor ratios on GQD properties, including size, fluorescence, and surface functionality. By optimizing these ratios, it is possible to tailor GQDs for diverse applications, from high-fluorescence bioimaging probes to selective chemical sensors and efficient energy materials.

This study addresses this gap by synthesizing GQDs through the pyrolysis of citric acid, phenylalanine, and tryptophan, with systematically varied ratios to evaluate their influence on synthesis efficiency and material properties. Characterization techniques such as UV-Vis spectroscopy, fluorescence spectroscopy, Fourier-transform infrared (FTIR) spectroscopy, and zeta size distribution and zeta potential analysis using a Zetasizer were employed to examine the structural and optical properties of the synthesized GQDs. Key parameters such as quantum yield, particle size distribution, and functional group composition were analyzed to identify the optimal precursor ratio. The findings not only provide insights into the precursor-property relationship but also offer guidance for the rational design of GQDs with enhanced performance

for specific applications. By shedding light on the interplay between precursor composition and GQD properties, this work advances the field of nanomaterial synthesis and paves the way for the development of customized GQDs for applications in bioimaging, environmental sensing, energy conversion, and beyond.

#### **MATERIAL AND METHODS**

#### **Materials and Instrumentation**

The synthesis of Graphene Quantum Dots (GQDs) was carried out using citric acid (CA), phenylalanine (Phe), and tryptophan (Trp) as precursors, all of which were of analytical grade and used without further purification. Citric acid, obtained from Sigma-Aldrich, served as the primary carbon source, while phenylalanine and tryptophan, also purchased from Sigma-Aldrich, provided nitrogen doping and aromatic functionalities to enhance the structural and optical properties of the GQDs. All solutions were freshly prepared using Milli-Q water (resistivity >18.2 M $\Omega$ ·cm) produced by a Milli-Q system (Millipore, USA). Characterization of the synthesized GQDs was performed using a UV-Vis spectrophotometer (Shimadzu UVmini-1240), a fluorescence spectrophotometer (Shimadzu RF-5301PC), and a Fourier-transform infrared (FTIR) spectrometer (PerkinElmer Spectrum One, Nicolet 520). Additionally, the hydrodynamic diameter and zeta potential of the GQDs were determined using a Zetasizer Nano ZS (Malvern Panalytical, UK). All chemicals were stored under standard conditions, and appropriate safety measures, including the use of personal protective equipment (PPE), were strictly followed during handling.

#### **Method and Characterization**

Graphene Quantum Dots (GQDs) were synthesized via a pyrolysis method using citric acid as the primary carbon source and phenylalanine and tryptophan as nitrogendoping precursors, as described in our previous studies <sup>22-25</sup>. A specific ratio of citric acid, phenylalanine, and tryptophan was used as listed in Table 1. The precursors were added to a 10.0 mL beaker containing silicone oil and heated to 200°C on a hot plate. After approximately 10 minutes, the precursor mixture liquefied, and the color of the solution changed from colorless to pale yellow, indicating the formation of GQDs. The GQDs liquid was then transferred into 25 mL of Milli-Q water and stirred at 300 rpm to facilitate complete dispersion and further processing. Upon cooling, the GQDs solution was passed through a 0.22 µm membrane filter to eliminate large aggregates and impurities. After the synthesis of GQDs, the obtained yellow liquid was purified by liquidliquid extraction using tertiary butyl alcohol (TBA) to remove unreacted precursors and small by-products. The solution was then subjected to a freeze-drying process to obtain a dry powder of purified GQDs. The dried GQDs were stored at room temperature (20-25°C) in a desiccator protected from moisture for further characterization and analysis.

The synthesized GQDs were characterized to evaluate their structural, optical, and morphological properties. UV-Vis spectrophotometry (recorded in the range of 220 to 350 nm with a resolution of 1 nm using a 1 cm path length quartz cuvette) was employed to identify absorption peaks

associated with the  $\pi$ - $\pi^*$  transitions of aromatic sp² domains. Fluorescence spectrophotometry (excitation at 350 nm; emission recorded from 360 to 600 nm with a resolution of 1 nm) was used to analyze the photoluminescence properties, including emission wavelength and quantum yield. Fourier-transform infrared (FTIR) spectroscopy (scan range: 4000–400 cm³; resolution: 4 cm³) provided insights into the surface functional groups present on the material. Additional analyses included particle size distribution using dynamic light scattering (DLS) and zeta potential measurements to assess colloidal stability. These comprehensive characterizations provided a detailed understanding of the influence of precursor ratios on the physical and chemical properties of the GQDs.

**Table 1** The composition of Precursors and Their Ratios Used in the Synthesis of Graphene Quantum Dots (GQDs)

Name	CA, g	Phe, g	Trp, g
GQDs1	2.0	0.75	0.25
GQDs2	2.0	0.50	0.50
GQDs3	2.0	0.25	0.75

#### **RESULTS AND DISCUSSION**

FTIR analysis was used to characterize the synthesized GQDs from citric acid (CA), phenylalanine (Phe), and tryptophan (Trp). The spectra revealed several important features that provide insights into the chemical composition of the GQDs in Figure 1. All spectra, including those of citric acid, phenylalanine, tryptophan, and the GQDs, exhibited a broad stretching vibration of the amine N-H bond around 3360 cm<sup>-1</sup>. This indicates that amine groups are present in all three precursor compounds, with the highest intensity observed in the GQDs, suggesting a prominent presence of amine groups on the GQDs surface. The band at 3350 cm<sup>-1</sup> (Phe) and 3360 cm<sup>-1</sup> (Trp) reflects the N-H stretch, characteristic of amines in all components, which contribute to the functionalization of the GQDs. The C-H and C=C stretching vibrations in the GQD spectra, appearing around 3020 cm<sup>-1</sup> and 1580 cm<sup>-2</sup> 1, indicate the presence of graphene-like structures and confirm the formation of the GQDs. These bands reflect the sp<sup>2</sup>-hybridized carbon framework, typical of GQDs. A clear absorption band around 1740 cm<sup>-1</sup> is observed in the GQDs' spectra. The presence of carboxyl groups is confirmed by the C=O stretching vibrations around 1740 cm<sup>-1</sup> in all GQDs. The broad nature of this band, indicates the combination of C=O and amide C=O stretches, typical for carboxyl and amide groups. This suggests that phenylalanine and tryptophan residues are likely incorporated into the GQD structure, and the formation of amide bonds between the GQDs and these amino acids is evident. The carboxyl O-H stretching vibration around 3100 cm<sup>-1</sup> further confirms the presence of carboxyl groups, which are critical for increasing the solubility and functionalization of the GQDs. A shoulder around 1600 cm<sup>-1</sup> in the GQD spectra is observed, which corresponds to the N-H bending vibration, indicates that both phenylalanine and tryptophan contribute to the surface functionalization of the GQDs through interactions involving their amide and amine groups.

The C–H stretching vibrations observed around 2925 cm<sup>-1</sup> and 3020 cm<sup>-1</sup> in the GQDs' spectra further indicate the presence of alkyl and aromatic groups in the structure of the GQDs, which is likely due to the incorporation of both phenylalanine and tryptophan in the GQD framework.

The FTIR spectra suggest that the synthesized GQDs contain a combination of amine, carboxyl, amide, and aromatic functional groups, indicating the successful incorporation of citric acid, phenylalanine, and tryptophan into the GQDs' structure. The amine N-H stretching vibrations at 3360 cm<sup>-1</sup>, C-H stretching vibrations at 3020 cm<sup>-1</sup>, amide C=O stretches around 1700 cm<sup>-1</sup>, and carboxyl O-H stretches around 3100 cm<sup>-1</sup> demonstrate the presence of functional groups that are likely to enhance the reactivity, solubility, and potential for further modification of the GQDs. The increase in the amide bands and aromatic vibrations in GQDs2 and GQDs3, compared to GQDs1, reflects the influence of phenylalanine and tryptophan on the structure and surface chemistry of the GQDs. These results prove that the GQDs have been successfully functionalized and that the incorporation of amino acids alters the chemical structure, which may impact their applications in sensors, drug delivery, or other biomedical fields.

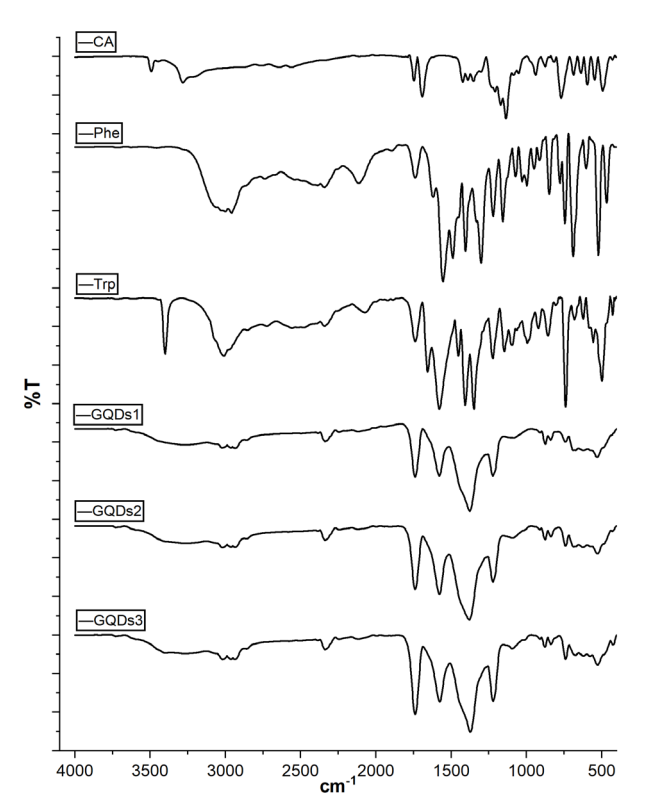


**Figure 1** FTIR spectra of citric acid (CA), phenylalanine (Phe), tryptophan (Trp), and GQDs synthesized from CA, Phe, and Trp.

The zeta potential measurements of the GQDs in deionized water revealed a decreasing trend with increasing tryptophan (Trp) content in Figure 2. GQDs1, GQDs2 and, GQDs3 exhibited zeta potentials of -21.4 mV, -12.2 mV, and -7.5 mV, respectively. This trend suggests that higher Trp content reduces the overall negative charge of the GQDs, likely due

to the presence of indole functional groups and aromatic rings, which may partially neutralize surface carboxyl (-COO<sup>-</sup>) groups from citric acid. Similar findings have been reported in the literature, where the incorporation of amino acid precursors affects the surface charge of GQDs by influencing the density of oxygen-containing functional groups and the degree of  $\pi$ - $\pi$  interactions on the carbon framework <sup>22,26</sup>. Furthermore, the zeta potential values observed indicate a transition from highly stable colloidal dispersions (for CArich GQDs) to less stable systems as Trp content increases, which could impact their interactions with biological and environmental matrices. These results highlight the critical role of precursor composition in tuning the surface charge and stability of amino acid-derived GQDs, aligning with previous studies on precursor-dependent surface modifications in carbon-based nanomaterials <sup>27</sup>.

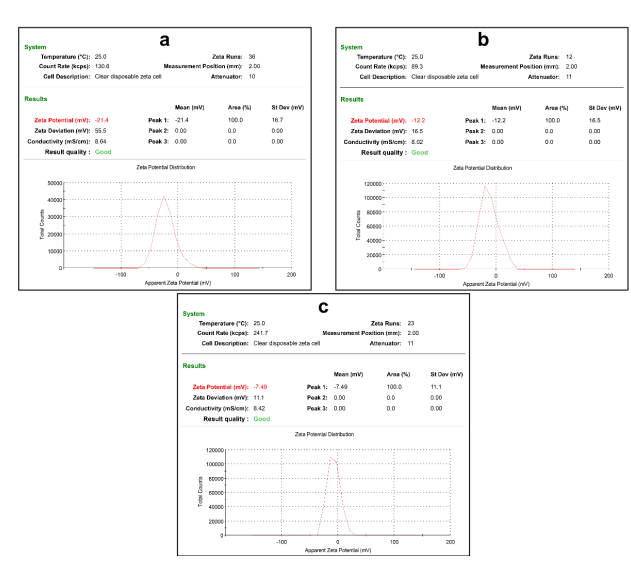


**Figure 2** Zeta potential measurements of GQDs in Milli-Q water: (a) GQDs1, (b) GQDs2, and (c) GQDs3.

The precursor composition significantly influenced the size distribution and polydispersity index (PDI) of the GQDs. The zeta size distributions of the GQDs are given in Figure 3. The size of the GQDs ranged from 0.89 nm to 1.5 nm, with only slight variation in size observed across the different precursor compositions. Specifically, GQDs1 exhibited the smallest size (0.89 nm) and the lowest PDI value (0.221), indicating more uniform particle distribution, GQDs2 had a slightly larger size (1.04 nm) with a PDI value of 0.312, suggesting a broader size distribution. GQDs3 showed the largest size (1.5 nm) and the highest PDI value (0.368), indicating the presence of more size variation within the sample. Although the overall change in size was modest, the precursor composition played a crucial role in controlling the size and PDI. The slight increase in size from GQDs1 to GQDs3 can be attributed to the varying amounts of tryptophan (Trp) and phenylalanine (Phe). Tryptophan, with its bulky indole ring, promotes larger carbon core formation, which contributes to the increased size in GQDs3. On the other hand, phenylalanine, with a smaller benzyl ring, encourages the formation of more compact and uniform GQDs, as seen in GQDs1. The GQDs2 resulted in a balance between the two amino acids, leading to

a slightly larger size (1.04 nm) and a broader size distribution (PDI 0.312). These results highlight that while the precursor composition influences the size distribution of GQDs, the overall change in size was not drastic, and the PDI values suggest that the GQDs with higher tryptophan content (such as GQDs3) tend to have more heterogeneous sizes. Although transmission electron microscopy (TEM) analysis was not performed in this study, the particle size values obtained from dynamic light scattering (DLS) measurements are in strong agreement with our previously reported TEM-based results for GQDs synthesized under comparable conditions using amino acid-derived precursors <sup>22,23,25</sup>. These studies confirmed that the GQDs synthesized through rapid pyrolysis typically exhibit sizes below 2 nm and possess low-crystalline. Based on these consistent findings and the current size range (0.89-1.5 nm), we anticipate that the particles in this study also share similar structural features. The presence of  $\pi$ -conjugated domains and functional aromatic residues further supports the formation of graphitic carbon frameworks even in the absence of direct lattice imaging. Therefore, the observed size data are considered reliable indicators of nanoscale GQD formation. The impact of precursor composition on the size and uniformity of GQDs is consistent with previous studies, where aromatic precursor selection and nitrogen functionalities have been shown to affect quantum dot nucleation, stability, and size control <sup>28,29</sup>.

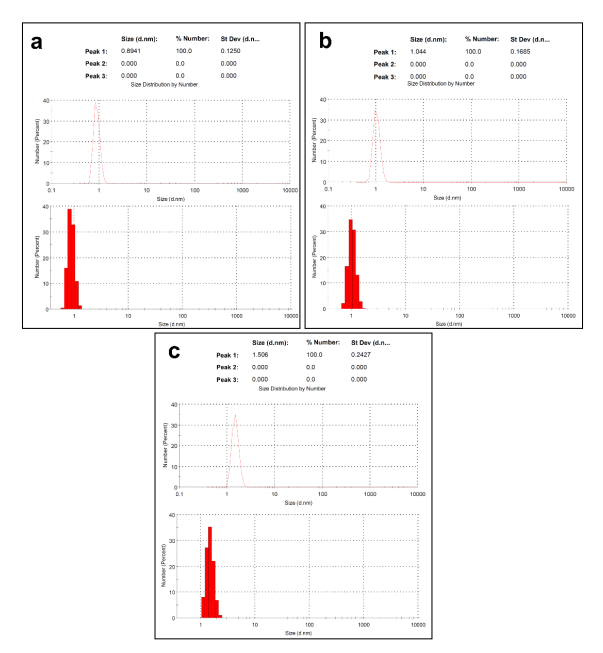


**Figure 3** Zeta size distribution of the synthesized GQDs with varying precursor compositions: (a) GQDs1, (b) GQDs2, and (c) GQDs3.

The UV-Vis absorption spectra (Figure 4a) of the GQDs exhibit characteristic peaks associated with  $\pi \to \pi^*$  (~230–270 nm) and  $n \to \pi^*$  (~300–350 nm) transitions <sup>18,30</sup>, with varying absorbance intensities among the samples (GQDs1, GQDs2, and GQDs3). The photoluminescence (PL) spectra (Figure 4b) reveal distinct emission profiles under UV excitation at 350 nm, where all GQD samples exhibit emission around 450 nm. GQDs2 demonstrate the highest fluorescence intensity, followed by GQDs3 and GQDs1. The inset images further

confirm the fluorescence behavior of the GQDs under UV light. These variations in optical properties indicate that the synthesis conditions significantly influence the electronic and emissive characteristics of GQDs, making them tunable for potential applications in sensing, bioimaging, and optoelectronic devices.

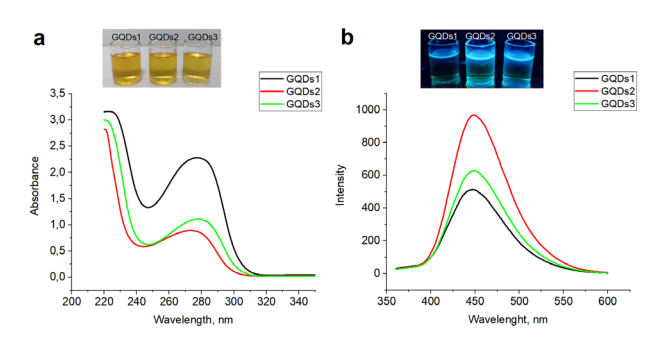


**Figure 4** Optical photographs of GQDs under daylight and 365 nm UV light (top), along with the absorbance (a) and fluorescence (b) spectra of GQDs synthesized with different precursor compositions.

The quantum yield (QY) was determined using quinine sulfate in  $0.10~M~H_2SO_4$  solution as the reference standard. The calculation was based on the following equation:

where  $\Phi$  represents the quantum yield, A represents the absorbance at the excitation wavelength, I denotes the integrated fluorescence intensity, and  $\eta$  refers to the solvent's refractive index. The subscripts "st" and "x" correspond to the standard (quinine sulfate) and the sample (synthesized GQDs), respectively. To ensure accurate comparison, GQDs solutions ( $\eta_x$  = 1.33) prepared under different synthesis conditions were diluted to maintain a consistent absorbance at 450 nm. Fluorescence spectra of these diluted samples were recorded within the 360–600 nm range upon excitation at 350 nm. The quantum yield calculations were performed using the reference value of  $\Phi_{st}$  = 0.54 for quinine sulfate in 0.10 M H<sub>2</sub>SO<sub>4</sub> ( $\eta_{cs}$ = 1.33).

The quantum yield (QY) of the GQDs was significantly influenced by the precursor composition, particularly the ratio of phenylalanine (Phe) and tryptophan (Trp). The QY of the synthesized GQDs was determined to be 32.2%, 95.5%, and 75.6% for GQDs1, GQDs2, and GQDs3, respectively. The sample with a higher Phe content (GQDs1) exhibited the lowest QY, likely due to lower nitrogen doping and reduced functionalization, resulting in fewer emissive states. In contrast, the Trp-rich sample (GQDs3) showed an increased QY, as the indole ring of Trp promotes enhanced  $\pi$ -electron delocalization and nitrogen incorporation, which can improve fluorescence efficiency. However, excessive nitrogen doping may introduce non-radiative recombination centers, limiting the QY improvement. The GQDs2 yielded the highest QY, suggesting an optimal balance between nitrogen incorporation and structural integrity. These findings align with previous studies reporting that nitrogen doping enhances QY, but excessive defects can act as quenching sites, reducing fluorescence efficiency <sup>26,31</sup>. Moreover, studies have shown that precursor selection and doping strategies significantly impact the optoelectronic properties of GQDs

<sup>32,33</sup>. These results provide valuable insights into tailoring GQD fluorescence properties for various optoelectronic and bioimaging applications.

To address concerns regarding the pyrolysis duration and structural development of the synthesized GQDs, it is important to note that short-term pyrolysis using amino acid precursors has been reported as an effective approach in recent studies. Our previous research demonstrated that nitrogen-rich amino acids such as glutamic acid and aspartic acid could yield GQDs with strong fluorescence within short reaction times <sup>23</sup>. Similarly, in our earlier work involving molecularly imprinted nanoparticles synthesized via a similar thermal method, we confirmed high quantum yield and structural integrity using only 10–15 minutes of pyrolysis <sup>22,23</sup>. Although conventional hydrothermal carbonization typically employs long heating durations, the use of highly reactive precursors such as citric acid and tryptophan significantly accelerates the carbonization and nitrogen doping process. This reactivity allows the formation of graphitic or partially crystalline carbon domains under rapid thermal exposure. Moreover, FTIR data and strong blue emission observed under UV excitation (365 nm) confirm successful formation of emissive structures. Literature also supports the formation of amorphous or low-crystalline GQDs without the need for extended high-temperature processing 18.

To provide a comprehensive contextualization of the findings, a comparative summary table (Table 2) has been incorporated, presenting key parameters such as quantum yield, precursor composition, and synthesis methodology reported in recent literature. This comparative analysis highlights both the effectiveness and the originality of the rapid pyrolysis method employed in this study, which utilizes a unique ternary precursor combination of citric acid, phenylalanine, and tryptophan. The results reinforce the importance of precursor engineering in the development of high-performance GQDs with tunable physicochemical properties.

Table 2 The comparison of selected GQDs studies

Precursor(s)	Methods	Size (nm)	Quantum Yield (%)	Ref.
Citric acid	Pyrolysis	~15	9.0	18
Citric acid and urea	Infrared- assisted pyrolysis	5.0-10.0	22.2	20
Citric acid and L-phenyl alanine	Hydrothermal	1.25-3.5	36.5	28
L-glutamic acid	Pyrolysis	4.66±1.24	54.5	34
Citric acid	Pyrolysis	0.7-1.0	11.5	35
Citric acid and glycine	Hydrothermal	3.0-8.0	~23	36
Citric acid, L-Phenyl alanine and L-Tryptophan	Pyrolysis	0.89-1.5	32.2-99.5	This study

#### CONCLUSION

This study demonstrated the successful synthesis of GQDs using citric acid, phenylalanine, and tryptophan as precursors, with systematic investigations into their structural, optical, and physicochemical properties. The results highlighted that the precursor composition significantly influenced the size distribution, surface charge, and fluorescence efficiency of the synthesized GQDs. FTIR analysis revealed the presence of key functional groups, including -OH and -COOH, as well as aromatic C=C and C-N bonds, confirming successful functionalization and nitrogen doping. The particle sizes remained within a narrow range (0.89-1.5 nm), with increasing tryptophan content leading to slightly larger sizes and broader distributions. Additionally, zeta potential measurements indicated a gradual decrease in surface charge with higher tryptophan content, confirming changes in surface chemistry and colloidal stability. Optical characterization revealed strong absorbance and fluorescence properties, with distinct  $\pi \rightarrow \pi^*$  and  $n \rightarrow \pi^*$  transitions in the UV-Vis spectra. Fluorescence quantum yield (QY) analysis further confirmed that nitrogen incorporation played a key role in tuning optical efficiency, where an optimal balance between phenylalanine and tryptophan (GQDs2) resulted in the highest QY (95.5%). In contrast, excessive nitrogen doping led to fluorescence quenching, underscoring the importance of controlled precursor selection. Overall, the study provides valuable insights into tailoring GQD properties through precursor engineering. The tunability of size, charge, and fluorescence characteristics offers potential for application in optoelectronics, bioimaging, and chemical sensing. Further studies are needed to explore the scalability of the synthesis method and the real-world performance of the GQDs in practical applications, including environmental monitoring and drug delivery.

#### **Acknowledgement**

The author received no financial support for the research, authorship, and/or publication of this article.

#### References

- Cui Y, Liu L, Shi M, Wang Y, Meng X, Chen Y, et al. A review of advances in graphene quantum dots: from preparation and modification methods to application. C-J. Carbon Res. 2024;10(1):7.
- Iravani S, Varma RS. Green synthesis, biomedical and biotechnological applications of carbon and graphene quantum dots. A review. Environ. Chem. Lett. 2020;18:703-727.
- Yan Y, Gong J, Chen J, Zeng Z, Huang W, Pu K, et al. Recent advances on graphene quantum dots: from chemistry and physics to applications. Adv. Mater. 2019;31(21):1808283.
- Zheng XT, Ananthanarayanan A, Luo KQ, Chen P. Glowing graphene quantum dots and carbon dots: properties, syntheses, and biological applications. Small. 2015;11(14):1620-1636.
- 5. Chung S, Revia RA, Zhang M. Graphene quantum dots and their applications in bioimaging, biosensing, and therapy. Adv. Mater. 2021;33(22):1904362.
- Ghaffarkhah A, Hosseini E, Kamkar M, Sehat AA, Dordanihaghighi S, Allahbakhsh A, et al. Synthesis, applications, and prospects of graphene quantum dots: a comprehensive review. Small. 2022;18(2):2102683.
- 7. Hung YC, Wu J-R, Periasamy AP, Aoki N, Chuang C. Advances

- in spin properties of plant leaf-derived graphene quantum dots from materials to applications. Nanotechnology. 2025.
- Rodríguez-Caicedo JP, Joya-Cárdenas DR, Corona-Rivera MA, Saldaña-Robles N, Damian-Ascencio CE, Saldaña-Robles A. Efficiency of Graphene Quantum Dots in Water Contaminant Removal: Trends and Future Research Directions. Water. 2025;17(2):166.
- Sharma P, Yadav P, Kumar A, Mudila H. Exploration of graphene quantum dots: Design, properties, energy storage and conversion. J. Power Sources. 2025;630:236177.
- Das N, Srivastava R, Roy S, De AK, Kar RK. Physico-chemical properties and biological evaluation of graphene quantum dots for anticancer drug susceptibility. Colloids Surf. B: Biointerfaces. 2025;245:114322.
- Saeidi S, Rezaei B, Irannejad N, Ensafi AA. Efficiency improvement of luminescent solar concentrators using upconversion nitrogen-doped graphene quantum dots. J. Power Sources. 2020;476:228647.
- Huang C-L, Huang C-C, Mai F-D, Yen C-L, Tzing S-H, Hsieh H-T, et al. Application of paramagnetic graphene quantum dots as a platform for simultaneous dual-modality bioimaging and tumor-targeted drug delivery. J. Mater. Chem. B. 2015;3(4):651-664
- Anusuya T, Kumar V, Kumar V. Hydrophilic graphene quantum dots as turn-off fluorescent nanoprobes for toxic heavy metal ions detection in aqueous media. Chemosphere. 2021;282:131019.
- Balkanloo PG, Sharifi KM, Marjani AP. Graphene quantum dots: Synthesis, characterization, and application in wastewater treatment: A review. Mater. Adv. 2023;4(19):4272-4293.
- Haque E, Kim J, Malgras V, Reddy KR, Ward AC, You J, et al. Recent advances in graphene quantum dots: synthesis, properties, and applications. Small Methods. 2018;2(10):1800050.
- Tian P, Tang L, Teng K, Lau S. Graphene quantum dots from chemistry to applications. Mater. Today Chem. 2018;10:221-258.
- Kadyan P, Malik R, Bhatia S, Al Harrasi A, Mohan S, Yadav M, et al. Comprehensive review on synthesis, applications, and challenges of graphene quantum dots (GQDs). J. Nanomater. 2023;2023(1):2832964.
- Dong Y, Shao J, Chen C, Li H, Wang R, Chi Y, et al. Blue luminescent graphene quantum dots and graphene oxide prepared by tuning the carbonization degree of citric acid. Carbon. 2012;50(12):4738-4743.
- Bezuneh TT, Fereja TH, Li H, Jin Y. Solid-phase pyrolysis synthesis
  of highly fluorescent nitrogen/sulfur codoped graphene
  quantum dots for selective and sensitive diversity detection of
  Cr (VI). Langmuir. 2023;39(4):1538-1547.
- Gu S, Hsieh C-T, Yuan C-Y, Gandomi YA, Chang J-K, Fu C-C, et al. Fluorescence of functionalized graphene quantum dots prepared from infrared-assisted pyrolysis of citric acid and urea. J. Lumin. 2020;217:116774.
- 21. Sweetman MJ, Hickey SM, Brooks DA, Hayball JD, Plush SE. A practical guide to prepare and synthetically modify graphene quantum dots. Adv. Funct. Mater. 2019;29(14):1808740.

- Üzek R, Sari E, Şenel S, Denizli A, Merkoçi A. A nitrocellulose paper strip for fluorometric determination of bisphenol A using molecularly imprinted nanoparticles. Mikrochim. Acta. 2019;186:1-10.
- Sari E, Uzek R, Merkoci A. Paper based photoluminescent sensing platform with recognition sites for tributyltin. ACS sensors. 2019;4(3):645-653.
- Bal FB, Sari E, Üzek R, Loğoğlu E. Nanocomposite as visible sensing platform for Hg<sup>2+</sup>. IEEE Sens. J. 2021;21(9):10595-10602.
- 25. Üzek R. Engineering a Graphene Quantum Dot-Enhanced Surface Plasmon Resonance Sensor for Ultra-Sensitive Detection of Hg2<sup>+</sup> Ions. Adv. Mater. Interfaces. 2025;12(5):2400679.
- Sari E. Synthesis and characterization of high quantum yield graphene quantum dots via pyrolysis of glutamic acid and aspartic acid. J. Nanoparticle Res. 2022;24(2):37.
- Li L, Li L, Wang C, Liu K, Zhu R, Qiang H, et al. Synthesis of nitrogen-doped and amino acid-functionalized graphene quantum dots from glycine, and their application to the fluorometric determination of ferric ion. Mikrochim. Acta. 2015;182:763-770.
- Kostromin S, Borodina A, Pankin D, Povolotskiy A, Bronnikov S. N-doped carbon quantum dots obtained from citric acid and L-phenylalanine. Chem. Phys. Lett. 2024;841:141175.
- Ruiyi L, Sili Q, Zhangyi L, Ling L, Zaijun L. Histidine-functionalized graphene quantum dot-graphene micro-aerogel based voltammetric sensing of dopamine. Sens. actuators B Chem. 2017;250:372-382.
- Moon BJ, Kim SJ, Lee A, Oh Y, Lee S-K, Lee SH, et al. Structurecontrollable growth of nitrogenated graphene quantum dots via solvent catalysis for selective CN bond activation. Nat. Commun. 2021;12(1):5879.
- Li M, Tang N, Ren W, Cheng H, Wu W, Zhong W, et al. Quenching of fluorescence of reduced graphene oxide by nitrogen-doping. Appl. Phys. Lett. 2012;100(23).
- 32. Nguyen KG, Huš M, Baragau I-A, Puccinelli E, Bowen J, Heil T, et al. Controlling the optoelectronic properties of nitrogen-doped carbon quantum dots using biomass-derived precursors in a continuous flow system. Carbon. 2024;230:119623.
- Shi L, Wang B, Lu S. Efficient bottom-up synthesis of graphene quantum dots at an atomically precise level. Matter. 2023;6(3):728-760.
- 34. Wu X, Tian F, Wang W, Chen J, Wu M, Zhao JX. Fabrication of highly fluorescent graphene quantum dots using L-glutamic acid for in vitro/in vivo imaging and sensing. Journal of Materials Chemistry C. 2013;1(31):4676-4684.
- Wang S, Chen Z-G, Cole I, Li Q. Structural evolution of graphene quantum dots during thermal decomposition of citric acid and the corresponding photoluminescence. Carbon. 2015;82:304-313
- Ke Y, Liu YC, Ren WW, Bai AM, Li XY, Hu YJ. Preparation of graphene quantum dots with glycine as nitrogen source and its interaction with human serum albumin. Luminescence. 2021;36(4):894-903.